

Are your **MRI contrast agents** cost-effective?

Learn more about generic **Gadolinium-Based Contrast Agents**.



FRESENIUS
KABI

caring for life

AJNR

Use of computerized CT analysis to discriminate between Alzheimer patients and normal control subjects.

T Sandor, M Albert, J Stafford and S Harpley

AJNR Am J Neuroradiol 1988, 9 (6) 1181-1187

<http://www.ajnr.org/content/9/6/1181>

This information is current as of April 19, 2024.

Use of Computerized CT Analysis to Discriminate Between Alzheimer Patients and Normal Control Subjects

Tamas Sandor¹
 Marilyn Albert²
 Juliene Stafford³
 Sarah Harpley¹

A newly developed computerized technique was used to analyze the CT scans of 49 patients with dementia of the Alzheimer type and 31 normal control subjects. Nine brain regions distributed across five CT slices were evaluated for each individual. For the purpose of analysis, the patients and controls were divided into an exploratory set and a test set. Several discriminant functions were conducted on the exploratory set and applied to the test set. The combination of variables that focused on regions in the temporal lobe was most accurate in differentiating Alzheimer patients from controls (94%). This degree of accuracy was achieved only when subjects younger than 65 years old were analyzed separately from those 65 years old and older.

The newly developed computer software program was able to discriminate between independently selected groups of Alzheimer patients and control subjects. The program was most effective when the analysis emphasized regions in the temporal lobe and when subjects younger than 65 years old were analyzed separately from those 65 years old and older.

A number of CT studies have concluded that computerized measures of CT scans in patients with dementia of the Alzheimer type are significantly different from those of control subjects [1-5]. Some have demonstrated an accuracy of correct classification as high as 93%.

However, it is unclear whether the accuracy of any of these measurement procedures can be replicated in a second group of independently selected subjects. This is an important goal because, to be useful in identifying patients with Alzheimer disease, any measurement technique must have sensitivity. To be sensitive, a procedure must differentiate between patients and controls with a high degree of accuracy in groups of independently selected subjects.

The focus of our current study was to evaluate a newly developed computer-assisted image-analyzing technique with regard to measurement sensitivity. The new computerized technique was developed to reduce measurement variability related to partial-volume effects and beam-hardening. Partial volume refers to the fact that while some pixels are all tissue or all fluid, others are only partially tissue and partially fluid. Beam-hardening manifests itself in the so-called cupping effect, which refers to the increase in CT numbers near the periphery of the CT slice [6, 7]. A computer program that can reduce this artifact can segment the pixels into fluid and tissue regions with greater accuracy, particularly at the skull-brain boundary. This may improve the ability to distinguish between Alzheimer patients and control subjects.

To improve diagnostic accuracy it is important to focus on the regions of the brain that are known to reflect the primary neuropathologic change of the disorder in question. With regard to Alzheimer disease, it is increasingly clear that regions in the temporal lobe are of primary importance. This includes the hippocampus, the amygdala, and the parahippocampal gyri of the medial temporal region, as well as the medial and inferior temporal gyri and the posterior ends of the sylvian fissure [8-13]. If microscopic changes in these areas are reflected in macroscopic altera-

Received September 28, 1987; accepted after revision April 4, 1988.

This work was supported in part by grant PO1-AG04953 from the National Institute of Aging, by grant PO1-CA32849 from the National Institutes of Health, and by funds from AG Siemens and the Unicure Foundation.

¹Department of Radiology, Brigham & Women's Hospital, Harvard Medical School, Boston, MA 02115.

²Departments of Psychiatry and Neurology, Massachusetts General Hospital, Division on Aging, Harvard Medical School, Boston, MA 02114. Address reprint requests to M. Albert, Department of Psychiatry, Massachusetts General Hospital, Boston, MA 02114.

³Department of Psychiatry, University of Rochester Medical School, Rochester, NY 14603.

AJNR 9:1181-1187, November/December 1988
 0195-6108/88/0906-1181

© American Society of Neuroradiology

tions in the atrophic characteristics of the tissue, measurements of these regions should improve one's ability to differentiate Alzheimer patients from controls. A recent study that used perceptual ratings of CT scans confirmed this hypothesis by demonstrating that the identification of Alzheimer patients was improved when atrophy ratings of temporal-lobe regions were emphasized [14]. Computerized measures of these regions should further increase patient identification.

Our current study was undertaken to determine the degree to which the CT scans of several groups of Alzheimer patients and controls could be differentiated by the newly developed computerized procedure that incorporated measurements of temporal-lobe regions. Comparisons were made separately for subjects younger and older than 65 years of age, as well as for all subjects together, because previous studies have indicated that the variables that distinguish younger and older Alzheimer patients from controls differ [3, 4].

Subjects and Methods

Subjects

Eighty subjects were included in the study, 49 patients with dementia of the Alzheimer type and 31 normal control subjects. They were 51–82 years old. The mean age of the Alzheimer patients was 69.3 ± 8.6 and the mean age of the controls was 66.5 ± 7.6 . There was no significant difference in the ages of the two groups [$t(2, 78) = 1.48, p = .14$].

The diagnosis of Alzheimer disease was made in concordance with National Institute of Neurological and Communication Disorders and Stroke/Alzheimer's Disease and Related Disorders Association criteria [15]. It was based on the judgment of a staff neurologist, with independent agreement from a staff psychiatrist and neuropsychologist. Several diagnostic tests (e.g., CT, electroencephalography, 12-factor automated blood chemistry test, urinalysis, and measurement of thyroxine and folate levels) were administered to exclude those patients with medical conditions known to produce dementia. These tests were used to rule out various hydrocephalic, metabolic, neoplastic, infectious, and traumatic causes of dementia. Patients with a record of severe head trauma, alcoholism, serious psychiatric illness, learning disabilities, epilepsy, lung disease, kidney disease, or cancer were excluded. All Alzheimer patients received an ischemic score of 4 or less on the ischemic scale for estimating the likelihood of multifactor dementia [16].

The normal controls were members of the Normative Aging Study at the Boston Veterans Administration Outpatient Clinic. As such, complete medical records were available on these individuals for the past 20 years. Subjects with a history of alcoholism, psychiatric illness, epilepsy, chronic lung disease, kidney disease, or cancer were excluded from this study.

All subjects provided informed consent for study participation.

CT Scan Assessment

CT scans (without contrast material) were obtained with an Ohio-Nuclear Delta 2010 scanner at the Boston Veterans Administration Medical Center and a Somatom 2 CT scanner at the Brigham and Women's Hospital, Boston. The picture element size was 1×1 mm, and the image was reconstructed on a 256×256 matrix. The CT density number scale was -1000 for air (± 2 H) and 0 for water. The scans were obtained approximately 20° to the canthomeatal line starting at the level of the chiasmatic cistern and proceeding to the level of the superficial sulci at the vertex. Each CT slice was 7 mm

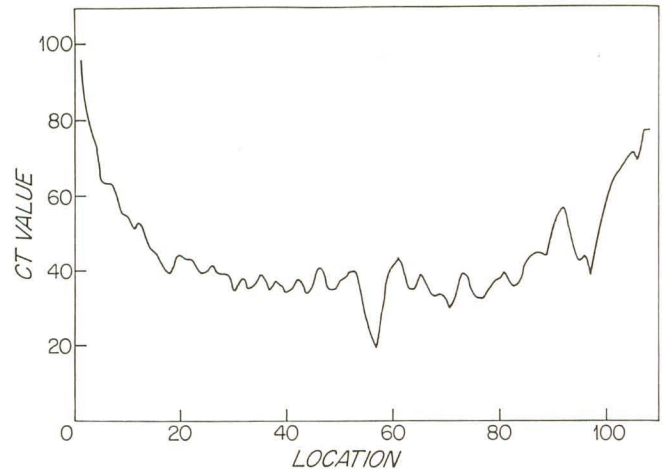


Fig. 1.—Graph of CT attenuation values shows cupping effect. Analysis was performed on slice at bodies of lateral ventricles.

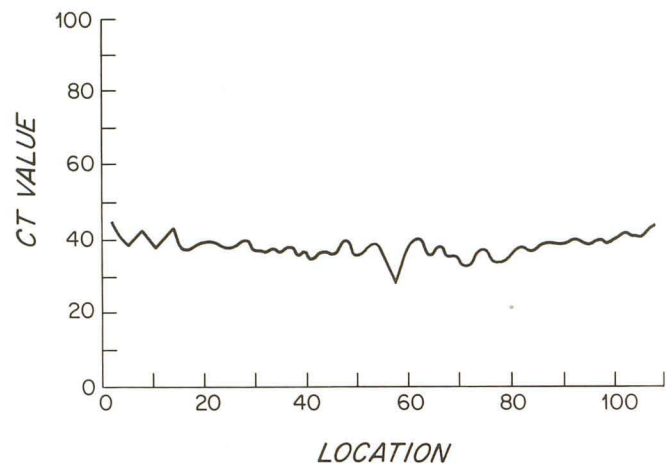


Fig. 2.—CT attenuation values after procedure to reduce cupping effect has been applied. Analysis was performed on slice at bodies of lateral ventricles.

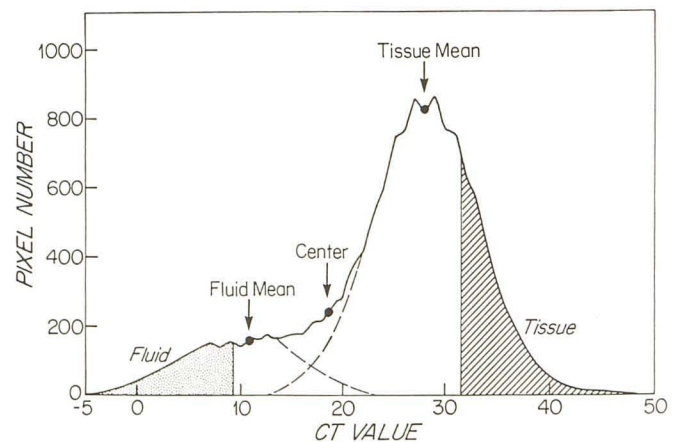


Fig. 3.—Example of regional distribution of CT attenuation values. Fluid mean, tissue mean, and center between the two distributions have been marked by the operator.

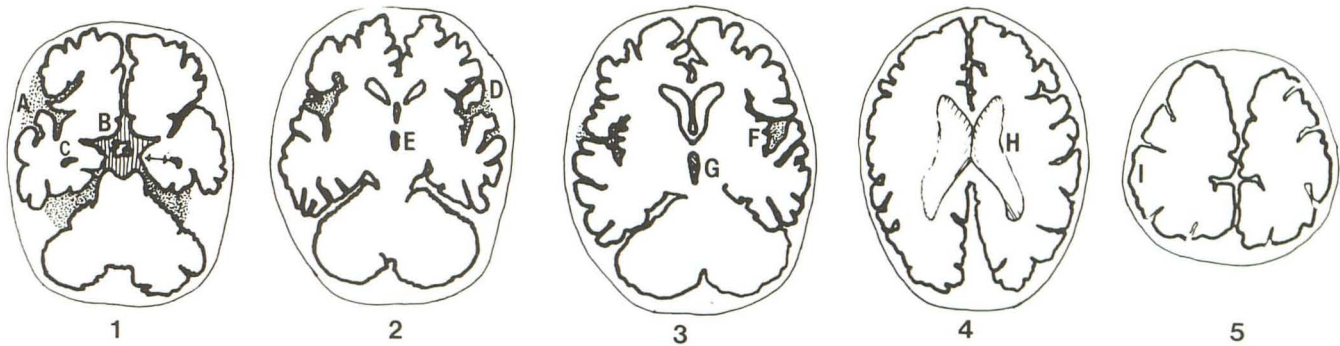


Fig. 4.—Five CT slices selected for evaluation.

Slice 1: A = sylvian fissures; B = suprasellar cistern; C = temporal horns of lateral ventricles.

Slice 2: D = sylvian fissures, E = third ventricle.

Slice 3: F = sylvian fissures, G = third ventricle.

Slice 4: H = bodies of lateral ventricles.

Slice 5: I = superficial sulci.

TABLE 1: Comparison of Computerized CT Measurements in Alzheimer Patients and Normal Control Subjects

CT Slice: Region	% Area (mean \pm SD)		Student's t Test
	Control	Alzheimer	
Slice 1:			
Sylvian fissure	1.7 \pm 0.7	3.3 \pm 1.4	-6.16
Temporal horn	0.2 \pm 0.2	1.1 \pm 0.8	-5.61
Suprasellar cistern	2.8 \pm 0.9	4.4 \pm 1.0	-7.03
Slice 2:			
Sylvian fissure	2.1 \pm 0.9	3.9 \pm 1.8	-6.73
Third ventricle	0.5 \pm 0.2	0.9 \pm 0.3	-6.49
Slice 3:			
Sylvian fissure	2.0 \pm 1.1	3.8 \pm 1.5	-5.77
Third ventricle	0.5 \pm 0.3	0.9 \pm 0.3	-5.24
Slice 4:			
Lateral ventricles	8.1 \pm 2.9	13.9 \pm 4.7	-6.10
Slice 5:			
Sulci	11.9 \pm 6.0	17.7 \pm 7.1	-3.83

Note.—These data are based on 49 Alzheimer patients and 31 normal control subjects (df = 78). There was a significant difference between the groups for each of the measurements ($p \leq .0001$).

thick. An approximately equal number of CT scans from patients and controls were obtained on each scanner.

The digitized CT data were stored on magnetic tape and transferred to a Microvax-2 computer. The images were displayed on a video monitor that permitted operator interaction with the displayed image.

A computer program, known as the Region Growing Program (Y. Kim, unpublished data), was used to determine the area of a region of interest. The program uses a three-step procedure to identify fluid and tissue in a given region. The first step is an automatic preprocessing algorithm that identifies all pixels within the cranium. The second step is also an automatic program that reduces the cupping effect in the CT image. The next step involves an operator-interactive program that identifies the fluid (i.e., CSF) and tissue regions (i.e., gray and white matter) on the scan.

The process of identifying the pixels within the skull has been described elsewhere [17]. The cupping effect can be illustrated by graphing the profile of CT values along a cut through the brain. Figure 1 indicates that the profile is cup-shaped; that is, the CT numbers near the periphery of the image are increased. The purpose of the

preprocessing algorithm is to level off these values so that they are fairly flat along the profile, as demonstrated in Figure 2. The preprocessing algorithm is applied to all CT slices where the region of interest occurs at or near the skull-brain boundary.

The operator-interactive program assumes that the image varies smoothly, and that fluid and tissue pixels are clustered together. The simplest and most common approach to identifying fluid and tissue on a CT slice is thresholding; that is, the use of fixed CT attenuation values as cutoff points. However, this would result in too many misclassifications. The current, more accurate method combines thresholding with a nearest-neighbor procedure. This latter method classifies a pixel on the basis of the CT attenuation values of the pixels that are adjacent to it. First, a determination is made of the CT values that clearly fall within the tissue or fluid range. This is accomplished by displaying the bimodal histogram of CT attenuation values for a region of interest. The operator then marks the mean of the fluid distribution, the mean of the tissue distribution, and the dip between the distributions (Fig. 3). Only pixels with CT numbers far removed from the overlap in the fluid and tissue distributions are classified in the first pass of the computation. These pixels are labeled as fluid or tissue. The remaining pixels are classified in the second pass, with the use of information from the pixels surrounding the pixel to be classified. To assess the reliability of the operator-interactive procedure, 12 CT scans were analyzed independently by two trained individuals.

Regions Selected for Evaluation

Five CT slices from each scan were selected for evaluation. These slices are shown in Figure 4. Nine regions of interest were selected. The area of the region of interest was normalized to the head size; that is, it was expressed in relation to the area as a whole, therefore, each value was termed percentage area. When the region existed in both hemispheres (i.e., the sylvian fissures, temporal horns, bodies of lateral ventricles, and superficial sulci), the percentages of the two areas were summed.

Results

Student's t Test

Student's t test was used to compare the percentage area for each of the selected features in the group of Alzheimer

TABLE 2: Percentage of CT Scans Correctly Classified (Alzheimer Patients vs Normal Control Subjects) by Discriminant Function Analysis of Exploratory Set and Test Set

Age of Group: Model No.	Region Selected (Slice No.)	% Correct		
		Mean	Exploratory Set	Test Set
<65 year old (n = 27):				
1	Temporal horn (1)	95	89	100
2	Sylvian fissures (2)	84	89	78
	Third ventricle (3)			
3	Lateral ventricle (4)	84	89	78
	Third ventricle (3)			
≥65 years old (n = 53):				
1	Suprasellar cistern (1)	92	89	94
2	Sylvian fissures (3)	82	89	75
	Third ventricle (3)			
3	Superficial sulci (5)	87	92	81
	Suprasellar cistern (1)			
All subjects (n = 80):				
1	Suprasellar cistern (1)	87	85	88
2	Temporal horn (1)	77	85	68
	Sylvian fissures (2)			
3	Third ventricle (2)	85	89	80
	Sylvian fissures (3)			
Suprasellar cistern (1)				
Third ventricle (2)				
Sylvian fissures (2)				

Note.—Model 1 focused on regions pertaining to the temporal lobe; model 2 focused on ventricular and supraventricular areas; and model 3 permitted the discriminant function to select from among all nine variables.

patients and in the control group. There was a significant difference between the groups for each of the measurements ($p \leq .0001$). Table 1 presents the results of this analysis.

Discriminant Function Analyses

Three sets of discriminant function analyses were performed. Set 1 included only subjects under the age of 65. The mean ages of the patients and controls in this set were 59.3 ± 3.9 and 59.0 ± 4.5 years, respectively. These means did not differ significantly from one another. Set 2 consisted of subjects 65 years old and older. The mean ages of the patients and controls in set 2 were 73.7 ± 5.9 and 71.2 ± 4.9 years, respectively. They also did not differ significantly in age. Set 3 combined all of the subjects, regardless of age, into one analysis. To determine whether the results of each of the analyses could be replicated in an independently selected group of subjects, the patients and controls in each set were randomly assigned to two subgroups—an exploratory set and a test set. The discriminant function analysis was then carried out on the exploratory set, and the discriminant coefficients from that analysis were applied to the test set.

Three models were examined within each set of discriminant functions: (1) *model 1* focused on regions pertaining to the temporal lobe; that is, measurements of the temporal horn, the suprasellar cistern, and the sylvian fissure on slices 1, 2, and 3; (2) *model 2* focused on ventricular and supraventricular areas; that is, measurements of the lateral ventricles,

the superficial sulci, and the third ventricle on slices 2 and 3; and (3) *model 3* permitted the discriminant function to select from among all nine of the variables. The results of these analyses are described below and are summarized in Table 2. Figures 5 and 6 show CT scans on which the regions that best discriminated between the patients and control subjects are outlined.

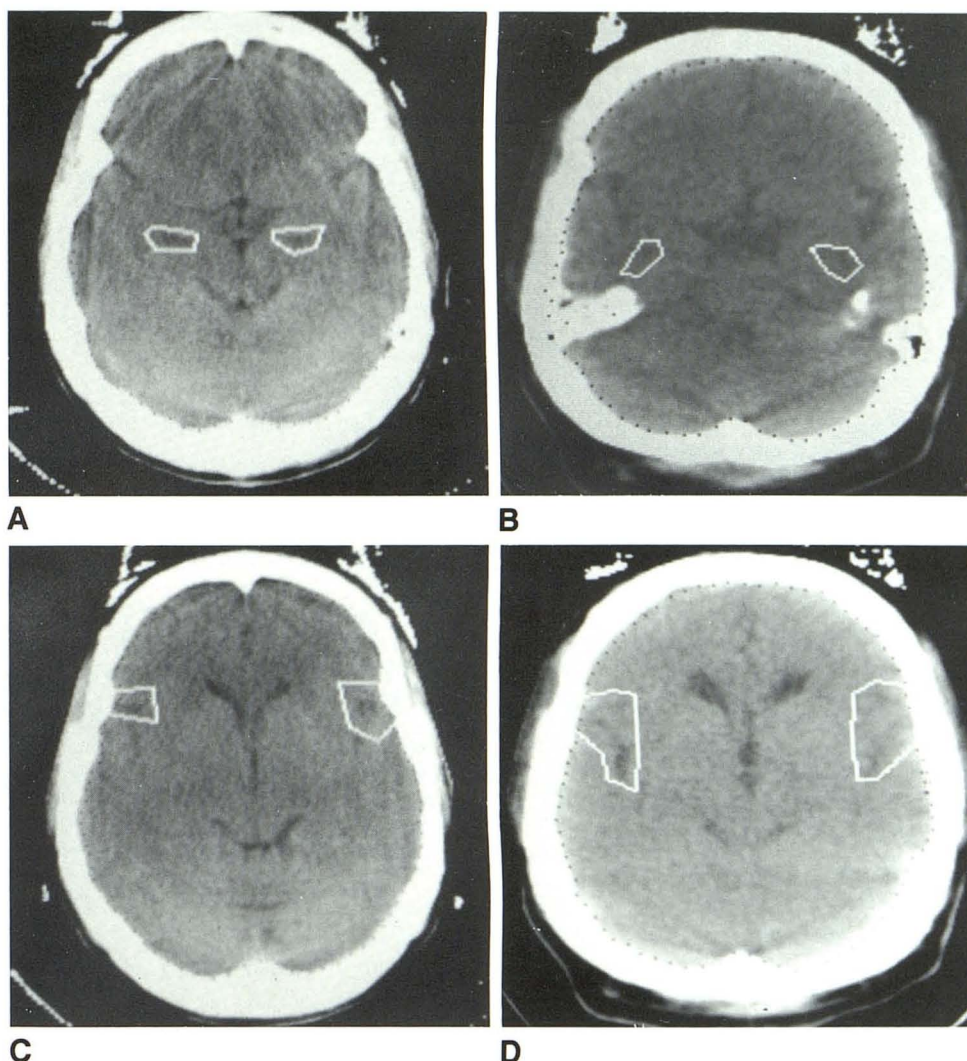
Subjects Under 65 Years of Age

Twenty-seven subjects were under 65 years of age. Eighteen were assigned to the exploratory set (normal controls, eight; Alzheimer, 10) and nine to the test set (normal controls, five; Alzheimer, four). For model 1, the discriminant function analysis selected two variables: the temporal horn on slice 1 and the sylvian fissure on slice 2. This discriminant function correctly classified 89% of the exploratory set and 100% of the test set [$\chi^2(3) = 11.434, p \leq .003$]. The average classification accuracy, therefore, was 95%. For model 2, the model that focused on ventricular and supraventricular regions, the discriminant function analysis selected two variables: the area of the third ventricle on slice 3 and the area of the lateral ventricles on slice 4. This discriminant function correctly classified 89% of the exploratory set and 78% of the test set [$\chi^2(2) = 13.086, p \leq .001$]. For model 3, the model that contained all variables, the discriminant function analysis selected the same two variables as model 2: the area of the third ventricle on slice 3 and the lateral ventricles on slice 4

Fig. 5.—CT scans of regions that best differentiate Alzheimer patients and controls younger than age 65. Photographs show manner in which regions are outlined before application of computer program.

A and B, Temporal horns on slice 1 in normal control subject (A) and Alzheimer patient (B).

C and D, Sylvian fissures on slice 2 in normal control subject (C) and Alzheimer patient (D).



$[\chi^2(2) = 13.773, p \leq .003]$. Thus, 89% of the exploratory set and 78% of the test set were correctly classified, for a mean of 84%.

Subjects 65 Years Old and Older

Fifty-three subjects were 65 years old or older. Thirty-seven were assigned to the exploratory group (normal controls, 12; Alzheimer, 25) and 16 to the test group (normal controls, seven; Alzheimer, nine). For model 1, the discriminant function selected two variables: the suprasellar cistern on slice 1 and the sylvian fissure on slice 3. This discriminant function correctly classified 89% of the exploratory set and 94% of the test set $[\chi^2(3) = 27.26, p \leq .00001]$. The average classification accuracy, therefore, was 92%. Three variables were selected for model 2: the sylvian fissure on slice 3, the third ventricle on slice 3, and the superficial sulci on slice 5 $[\chi^2(3) = 27.57, p \leq .00001]$. These variables classified 89% of the exploratory set and 75% of the test set correctly. Model 3 used three variables: the suprasellar cistern on slice 1, the third ventricle

on slice 3, and the superficial sulci on slice 5 $[\chi^2(3) = 32.26, p \leq .00001]$. This model correctly classified 92% of the exploratory group and 81% of the controls.

All Subjects

Of the 80 subjects in the study, 55 were assigned to the exploratory group (normal controls, 20; Alzheimer, 35) and 25 were in the test group (normal controls, 11; Alzheimer, 14). The discriminant function with model 1 selected three variables: the suprasellar cistern and the temporal horn on slice 1 and the sylvian fissure on slice 2 $[\chi^2(4) = 35.09, p \leq .00001]$. With these variables, 85% of the exploratory group and 88% of the test group were classified correctly. Model 2 selected the third ventricle on slice 2 and the sylvian fissure on slice 3 $[\chi^2(2) = 35.55, p \leq .00001]$. The exploratory group had an accuracy of 85% correct classification; that of the test group was 68%. Three variables were selected by model 3: the suprasellar cistern on slice 1 and the sylvian fissure and third ventricle on slice 2 $[\chi^2(3) = 38.69, p \leq .00001]$.

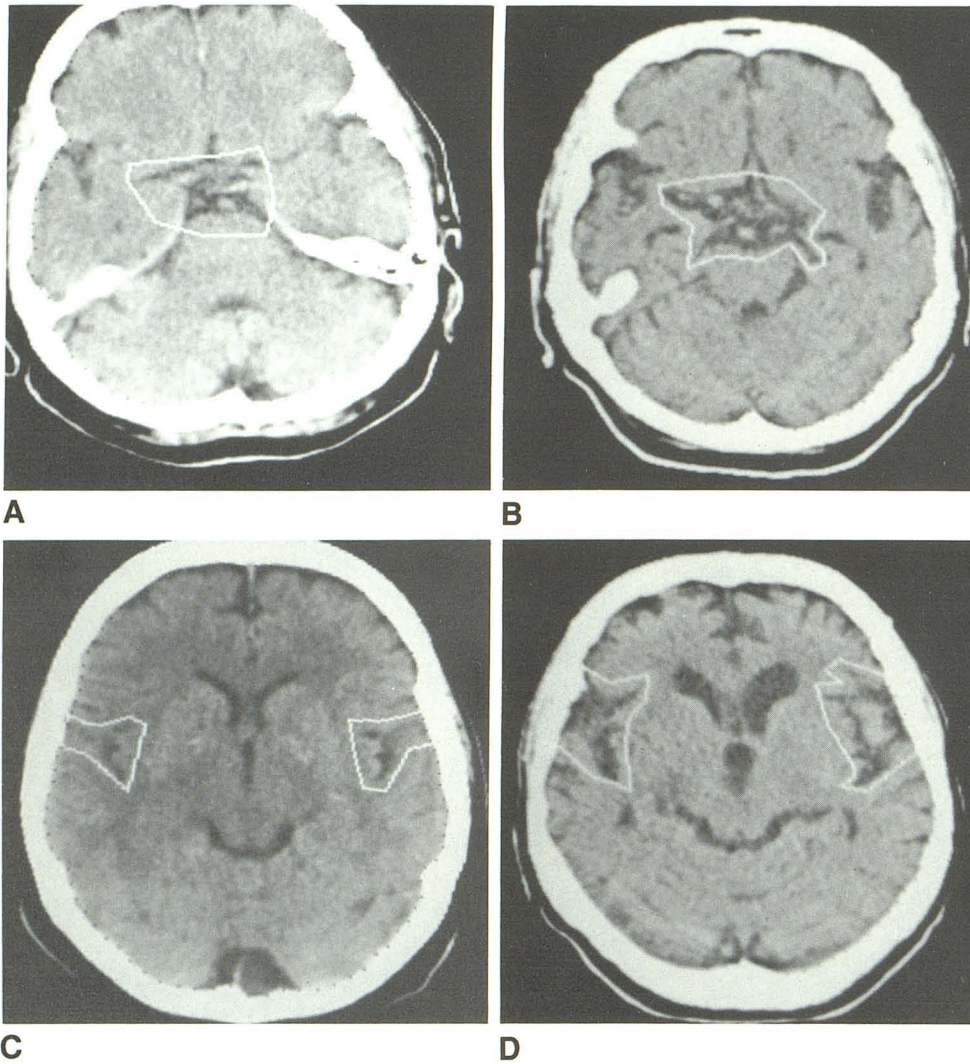


Fig. 6.—CT scans of regions that best differentiate Alzheimer patients and control subjects 65 years old and older. Photographs show manner in which regions are outlined before application of computer program.

A and B, Suprasellar cisterns on slice 1 in normal control subject (A) and Alzheimer patient (B).

C and D, Sylvian fissures on slice 3 in normal control subject (C) and Alzheimer patient (D).

Correlations

Pearson product moment correlations were used to evaluate the reliability with which the operator-interactive aspect of the Region Growing Program was implemented. The inter-correlations of seven of the nine measurements made by the two operators were calculated. Two regions on slice 2 were not included in the analysis because the same regions were represented on slice 3. Table 3 presents the results of the correlational analysis. Reliabilities ranged from .78 to .98 (mean, .92).

Discussion

The results indicate that the newly developed computerized procedure for analyzing CT scans (the Region Growing Program) can discriminate between independently selected groups of Alzheimer patients and controls with an average accuracy that approaches 94%. However, this degree of accuracy is achieved only when the analysis emphasizes regions in the temporal lobe, such as the temporal horn and

the Sylvian fissure, and when subjects under the age of 65 are analyzed separately from those 65 years old and older.

The average accuracy of the model that focused on regions in the temporal lobe was 95% for the younger subjects and 92% for the older subjects. However, this dropped to 87% when all of the subjects were combined in one analysis. The model that focused on ventricular and supraventricular areas had an average accuracy of 84% for the younger subjects and 82% for the older ones. When all the subjects were combined in one analysis, this model produced an average accuracy of 77%. Model 3, the model that used all variables, produced results that were lower than those of model 1 for both the younger (84%) and older (87%) subjects. When all the subjects were combined in one analysis, model 3 produced an accuracy that fell between those of models 1 and 2 (85%).

These findings support the conclusion of LeMay et al. [14] that the differentiation of Alzheimer patients from controls on CT scans is greatly improved by an assessment of regions in the temporal lobe. It is increasingly clear that the neuropathologic and neurochemical changes associated with Alzheimer disease are not evenly distributed. The temporal lobe is, on

TABLE 3: Intercorrelation of CT Measurements Performed by Two Independent Operators

CT Slice: Region	Correlation Coefficient (r)
Slice 1:	
Sylvian fissure	.78 ^a
Temporal horn	.98
Suprasellar cistern	.92
Slice 2:	
Sylvian fissure	.97
Third ventricle	.92
Slice 4:	
Lateral ventricles	.98
Slice 5:	
Sulci	.91

Note.— $n = 12$; $df = 10$.

^a $p \leq .003$; all others, $p \leq .0001$.

the whole, the most severely affected area. There is a concentration of neurofibrillary tangles in the pyramidal cells of the subicular area of the hippocampus [8]. Parts of the entorhinal cortex of the parahippocampal gyrus are also severely affected [10, 12], as well as the amygdala [9]. It has been suggested that these pathologic changes produce a functional isolation of the hippocampus, producing the memory impairment that typifies Alzheimer disease [12]. Because a striking memory deficit is the most common early symptom of Alzheimer disease [18], it is likely that these regions are affected early in the disease. Our current data indicate that a computerized analysis of CT scans in mildly impaired Alzheimer patients has a greater likelihood of accurately differentiating patients from controls if it is focused on the regions in the temporal lobe that are prominently affected by the disorder.

In addition, these data add to the increasing evidence that younger and older Alzheimer patients differ in a number of basic physiologic parameters. Late-onset cases show less widespread neuropathologic and neurochemical changes. They have fewer neurofibrillary tangles in the neocortex [19], less loss of cells in the nucleus basalis of Meynert [20], and a relatively pure cholinergic deficit confined to the temporal lobe and hippocampus [21]. By contrast, the early-onset cases have more extensive neuropathologic changes, along with abnormalities in several neurotransmitter systems [21, 22]. Therefore, it is not surprising that it is necessary to analyze the CT scans of younger and older Alzheimer patients separately to better differentiate Alzheimer patients from normal control subjects.

ACKNOWLEDGMENTS

We thank William Hanlon, Arthur D'Adamo, and Jennifer Reifel for assistance in processing the CT images and Kenneth Jones and Mary Hyde for guidance in the statistical analysis.

REFERENCES

- Gado M, Hughes CP, Danziger W, Chi D, Jost G, Berg L. Volumetric measurements of the cerebrospinal fluid spaces in demented subjects and controls. *Radiology* 1982;144:535-538
- Soininen R, Puranen M, Riekkinen PJ. Computed tomography findings in senile dementia and normal aging. *J Neurol Neurosurg Psychiatry* 1982;45:50-54
- Albert M, Naeser MA, Levine HL, Garvey AJ. Ventricular size in patients with presenile dementia of the Alzheimer's type. *Arch Neurol* 1984;41:1258-1263
- Albert M, Naeser MA, Levine HL, Garvey AJ. CT density numbers in patients with senile dementia of the Alzheimer's type. *Arch Neurol* 1984;41:1264-1269
- Creasey H, Schwartz M, Frederickson H, Haxby JV, Rapoport SI. Quantitative computed tomography in dementia of the Alzheimer type. *Neurology* 1986;36:1563-1568
- DiChiro G, Brooks RA, Dubal L, Chew E. The apical artifact: elevated attenuation values toward the apex of the skull. *J Comput Assist Tomogr* 1978;2:65-70
- Joseph P. Artifacts in computed tomography. In: Newton TH, Potts DG, ed. *Radiology of the skull and brain*, vol. 5. *Technical aspects of computed tomography*. St. Louis: Mosby, 1981:3956-3952
- Ball MJ, Fisman M, Hachinski V, et al. A new definition of Alzheimer's disease: a hippocampal dementia. *Lancet* 1985;1:14-16
- Herzog AG, Kemper T. Amygdaloid changes in aging and dementia. *Arch Neurol* 1980;37:625-629
- Hyman BT, Van Hoesen GW, Damasio AR, Barnes CL. Alzheimer's disease: cell-specific pathology isolates the hippocampal formation. *Science* 1984;225:1168-1170
- Kemper T. Neuroanatomical and neuropathological changes in normal aging and dementia. In: Albert ML, ed. *Clinical neurology of aging*. New York: Oxford University, 1984:9-52
- Hyman BT, Van Hoesen GW, Kromer LJ, Damasio AR. Perforant pathway changes and the memory impairment of Alzheimer's disease. *Ann Neurol* 1986;20:472-481
- Wilcock GK. The temporal lobe in dementia of the Alzheimer's type. *Gerontology* 1983;29:320-324
- LeMay M, Stafford JL, Sandor T, Albert M, Haykal H, Zamani A. Statistical assessment of perceptual CT scan ratings in patients with Alzheimer type dementia. *J Comput Assist Tomogr* 1986;10:802-809
- McKhann G, Drachman D, Folstein M, Katzman R, Price D, Stadlan E. Clinical diagnosis of Alzheimer's disease: report of the NINCDS-ADRDA work group under the auspices of Department of Health and Human Services Task Force on Alzheimer's Disease. *Neurology* 1984;34:939-944
- Hachinski J. Cerebral blood flow differentiation of Alzheimer's disease from multi-infarct dementia. In: Katzman R, Terry RD, Bick KL, eds. *Alzheimer's disease: senile dementia and related disorders*. New York: Raven, 1978:97-104
- Sandor T, Kido DK, Hanlon WB, Rumbaugh CL. Automated calvaria analysis from computerized axial tomographic scans. *Comput Biomed Res* 1981;14:119-124
- Albert M, Moss M. The assessment of memory disorders in patients with Alzheimer's disease. In: Squire L, Butters N, eds. *Neuropsychology of memory*. New York: Guilford, 1984:236-246
- Terry RD, Katzman R. Senile dementia of the Alzheimer type. *Ann Neurol* 1983;14:497-506
- Whitehouse PJ, Hedreen JC, Jones BE, Price DL. A computer analysis of neuronal size in nucleus basalis of Meynert in patients with Alzheimer's disease. *Ann Neurol* 1983;14:149-150
- Rossor MN, Iversen LL, Reynolds GP, Mountjoy CQ, Roth M. Neurochemical characteristics of early and late onset types of Alzheimer's disease. *Br Med J* 1984;288:961-963
- Cross AJ, Crow TJ, Perry EK, Perry RH, Blessed G, Tomlinson BE. Reduced dopamine-B-hydroxylase activity in Alzheimer's disease. *Br Med J* 1981;282:93-94